



# Predicting the risk of individual tree fall along powerlines in Norway with a mechanistic wind risk model and machine learning

Morgane Merlin<sup>1</sup>, Barry Gardiner<sup>2,3,4</sup>, Svein Solberg<sup>1</sup>

<sup>1</sup>Norwegian Institute for Bioeconomy Research (NIBIO), Division of Forestry and Forest Resources, Department of Forest Management, Høgskoleveien 8, 1433 Ås, Norway

<sup>2</sup>Institut Européen De La Forêt Cultivée, Cestas, France

<sup>3</sup>Department of Forestry Economics and Forest Planning, Albert- Ludwig- University Freiburg, Freiburg im Breisgau, Germany

<sup>4</sup>Forest Research, Northern Research Station, Roslin, Scotland, United Kingdom

10 *Correspondence to:* Morgane Merlin (morgane.merlin@nibio.no)

## Abstract.

Tree falls along linear infrastructures and in particular powerlines pose a significant economic, safety and environmental challenge for the companies and institutions managing these infrastructures. The quick progression and affordability of remote sensing technologies such as drone-based inventories offers the opportunity to quickly and efficiently map individual trees along these infrastructures, enabling precise vegetation management to reduce risks. Here, we show how the hybrid empirical and mechanistic wind risk model ForestGALES can be applied to assess the vulnerability of individual trees to windfalls along selected powerlines in southern Norway. The validation dataset contained 180 recorded individual tree falls along powerlines from the winter 2020-2021. There was no major wind event recorded that winter. However, still, the ForestGALES model performed adequately, with an AUC (area under the curve) of 0.67. Combining the vulnerability index from ForestGALES with all other available tree and environmental variables in a machine learning model (extreme gradient boost algorithm) did however significantly improve the prediction performance. These results highlight how a combination of high-quality remote sensing data at the individual tree level can be utilized with ForestGALES and machine learning to provide managers with high-resolution vulnerability information for vegetation management.

## 1 Introduction

25 Linear infrastructures such as roads, railways and powerlines are vital to our societies bringing important social and economic benefits. However, they often intersect with managed and unmanaged forested and other vegetated areas. Coupled with extreme weather events, vegetation-related damage on linear infrastructures poses important safety, social and economic risks. Tree monitoring and management to identify high-risk locations along linear infrastructures is key and a priority for proactive natural hazard and vegetation management (Gardiner et al., 2024; Poulos and Camp, 2010; Szymczak et al., 2022) also minimizing the footprint of these infrastructures on vegetation. Regarding power infrastructures and powerlines, global electricity demand has nearly doubled over the last two decades across the world and is set to continue



growing. The powerline grids are likely by 16 million new kilometres for the 2020-2030 period to connect all new sources of electricity across the world (IEA, 2020). This creates increasing pressure on forested lands and increased deforestation and fragmentation when new lines are laid out. In addition, a general aging of forests in Europe and more climatic disturbance 35 increase the problems (Patacca et al., 2022). Tree management is a significant growing need and expense for power transmission and distribution companies, for which traditional methods are rapidly becoming obsolete. The electricity distributors have a much larger area to manage the vegetation along the powerlines' right-of-way (ROW). They need to reduce tree fall risks while maintaining biodiversity, carbon sink strength, timber production and access for forest management among other ecosystem services.

40 The advent of new remote-based technologies paired with machine learning models is rapidly changing the methods for risk assessment and management planning for power suppliers (and for other linear infrastructures). Historically, utilities used a fixed cycle of ground-based patrols visually inspecting powerlines, a time-consuming and expensive routine task. The rapid development and dissemination of optical and LiDAR surveys of the powerlines with airplanes and drones has significantly upgraded the potential for extensive remote monitoring of the vegetation along powerlines (Walker and Dahle, 2023).  
45 Combined with new AI models and tools, these new technologies can provide the identification of individual trees and a detailed 3D representation of their characteristics such as species and size (Jain et al., 2021). The acquisition and processing of LiDAR data is however expensive and can be time-consuming, especially for large regions or countries with extensive network of distribution lines. Developing and applying existing and new models utilizing these datasets to quickly calculate vulnerability indices across large areas are therefore key for the electricity providers. This helps to move towards cost-  
50 effective precise and individual-based tree management in the powerline ROW by targeting sections with high vulnerability. It also offers the opportunity to increase the safety of ground crews, better comply with local regulations and policies, and optimize the planning process for new powerlines.

In this study, we applied the well-established forest wind damage risk model ForestGALES recently parameterized for Norwegian forests (Merlin et al., 2025). This is a hybrid empirical and mechanistic model for calculating the threshold 55 (Critical Wind Speed CWS) for wind damage for forest stands and individual trees (Gardiner et al., 2008; Hale et al., 2012, 2015), to a compiled drone-based dataset of individual trees along powerlines across southern and western Norway. The ForestGALES model provides a semi-mechanistic alternative to statistical damage models which have limited operational use, by incorporating the physical process of wind loading on individual trees in forests. In Norway, forests cover 38 % of the land and the high-voltage power grid stretches over 130,000 km. Power outages are in general scarce and short in  
60 Norway (e.g. in 2024 an end-user experienced an average of 1.7 power outages lasting more than 3 minutes, with one long-term power outage for an average of 3.5 hours (Avbrotsstatistikk fra Reguleringsmyndigheita for energi - NVE, 2025)), with 75% of them attributable to snow, ice, lightning, precipitation, wind and vegetation. However, stronger storms and heavier wet-snow events in recent years have directly and indirectly, via tree fall, impacted electricity delivery and financially burdened utilities and other involved parties (NVE, 2012). This includes severe cases of long-lasting outages for some  
65 consumers and indirect effects on other electricity-based facilities such as emergency networks. Widening of powerline gates



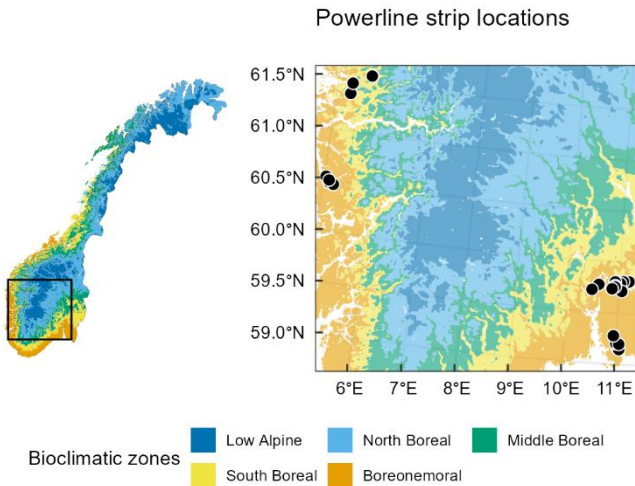
have been routinely carried out to secure powerlines against tree fall but may compromise forest cover, continuity and biodiversity. The utilities are therefore keen on implementing an operational solution collecting relevant data for predicting damage probability and design preventive and precise management. The objective of this study was thus to evaluate the performance of a Norwegian-parameterized version of ForestGALES for identifying trees at risk for wind damage along a  
70 given powerline.

## 2 Materials and Methods

In our study, we calculated CWS with ForestGALES for individual trees along selected powerline sections in southern Norway. To best represent the individual tree characteristics and the immediate forested environment, different seasonal (presence of snow on tree crowns) scenarios and definitions of tree variables (crown asymmetry, immediate tree  
75 neighbourhood definition) were used in the input dataset prior to the calculation of CWS by the ForestGALES model. This was to assess how to best define individual tree characteristics and local environment in order to obtain the most accurate damage predictions. Additionally, three alternative sources describing the wind climate were used when calculating the probability of damage. All options were evaluated for their performance in predicting tree damage against a validation dataset of recorded tree damage during the winter 2020-2021 and the best model selected.

### 80 2.1 Individual tree data

We used a single tree dataset from southern Norway (Fig. 1), i.e. mainly in the boreonemoral and south, boreal bioclimatic zones (Bakkestuen et al., 2008). It was compiled by eSmart Systems (<https://www.esmartsystems.com/>), a company providing AI-based services for the inspection and maintenance of energy infrastructures. The dataset contained single tree data along 25 forested powerline sections of 200 - 500 m in length and approximately 50 to 65 m in width, i.e. ~25 m on  
85 each side of the powerline gate. Out of the 25 locations, 17 were south of Oslo, and 8 were in the more northern and western region. Observations of individual tree damage in and around the 25 powerline locations (and a few observations in new locations – see Fig. 1) during the winter 2020-2021 (assumed due to wind damages; no heavy snow event were recorded for that period for the locations considered) were gathered early in summer 2021 and included both uprooted and broken trees. A total of 180 damaged trees were recorded, including 76 Norway spruce, 56 Scots pine and 48 broadleaved trees.



90

**Figure 1.** Maps showing the location of the study sites (black dots) within the larger study area in southern Norway (black rectangle) across the five bioclimatic regions of Norway.

The single tree data contained 18,689 trees, including 180 damaged trees (~1% of the full dataset). The acquisition of this dataset followed two main steps: first the acquisition of UAV laser scanning data and its pre-processing (for the 25 powerline strip locations), second the post-processing of this data to obtain all the required tree characteristics variables. A short description of both steps follows.

### 2.1.1 UAV laser scanning dataset

The field data collection took place across the summers 2020 and 2021. UAV laser scanning data were collected for the powerline strips. A base station with known GPS coordinates was used for accurate geocoding of the laser returns. The 100 collection was planned based on a 4 or 5 double line pattern along the powerline, at a flight altitude of ~60 m above ground and with a flight line spacing of ~10 m – 15 m, resulting in an overlap of the flight lines of ~85 % in front and ~75 % side and a scan angle of 0° from nadir, resulting in a ground sampling distance of near 1,41 cm/pixel. Several postprocessing engines were used but Pix4D (© 2025 Pix4D SA) and DroneDeploy (© 2025 DroneDeploy) were the major tools for this (details not shown). The pre-processing of the UAV-LS data yielded a dataset containing the coordinates, species, height and 105 the bounding box of each tree within 25 m of each side of the powerline gate. This pre-processed dataset underwent further processing to calculate the following “landscape” variables: the shortest distance from each tree to the powerline, the distance from each tree to the nearest forest edge (towards and away from the powerline or in the direction parallel to the powerline when an edge existed), the associated size of non-forested gaps (when present). The crown radii in the eight cardinal directions were measured to calculate the offset of the crown gravity centre relative to the top of the tree. The 110 diameter at breast height (DBH) was estimated using species-specific equations pairing UAV-LS-derived height data and field-based measurements of DBH (see Appendix A Table A1).



### 2.1.2 Tree data processing and final input dataset

The input dataset was then further processed to obtain all necessary variables required to calculate the CWS using ForestGALES. The stem volume and crown depth of each tree was estimated using Norwegian and species-specific 115 equations derived from the National Forest Inventory and described in the Appendix of Merlin et al. (2025). A measure of the crown asymmetry for each tree was done using the 8 crown radii measured in the previous step by estimating the displacement of the centre of gravity between a right circular cone shape and an irregular cone. Details about the calculation of the displacement of the crown centre of gravity are shown in Appendix A. The crown offset was then added in the calculation of the deflection loading factor (DLF) as an additional displacement of the crown weight – thereby increasing the 120 DLF compared to a tree with a symmetrical crown, decreasing the CWS thereby increasing the tree's vulnerability to wind damage (see Eq 2 and Eq 3 for the DLF in the CWS calculations, (Locatelli et al., 2022)).

For each tree, the characteristics of the surrounding trees were aggregated to represent the neighbourhood of each tree using Voronoi diagrams. We considered both the first order and second order neighbouring Voronoi cells – trees – when defining the neighbouring trees (hereafter named “tier 1 & tier 2”). We calculated the mean tree height, DBH, crown depth and width, 125 and distance for the neighbourhood trees and labelled this as stand variables. We calculated two competition indices , i.e. the Hegyi (distance-dependent, (Hegyi, 1974)) and the BAL (distance independent, (Stage, 1973)) . Both indices are implemented in the single-tree version of ForestGALES.

We derived soil type and rooting depth from the Geological Survey of Norway (NGU; [https://geo.ngu.no/kart/losmasse\\_mobil/](https://geo.ngu.no/kart/losmasse_mobil/)) and the ForestGALES classification (Kennedy, 2002) as detailed in the Appendix 130 of Merlin et al. (2025). Finally, we derived the topographic exposure index Topex (Chapman, 2000) from Norwegian elevation models at 10 m resolution across Norway for a horizon distance of 200, 500, and 1000 m averaged across the eight compass directions, hereafter referred to as Topex 200, Topex 500 and Topex 1000. Topex has been successfully used in forest wind damage assessments and modelling in complex terrain (Costa et al., 2023).

### 2.1.3 Characteristics of damaged and standing trees

135 A simple summary of the differences between the standing and damaged trees was performed for tree height, DBH, D/H ratio, the ratio of the estimated crown depth to tree height, species mix (whether the tree of interest was in a stand of the same species (coded 0), of a different species and a conifer species (coded 1), or of a different species and broadleaf (coded 2)), tree status (whether the tree of interest was taller or thinner than the neighbouring trees). Considering the large imbalance in the sample sizes between the damaged and standing trees, we used all the damaged trees (N = 180) and 140 performed the statistical tests for 100 simulations for a random selection of 180 standing trees with a similar species distribution as the damaged trees. Similar results were obtained when using the whole set of standing trees. The significance of the difference was tested using the Mann-Whitney-Wilcoxon (MWW) test foregoign assumptions about the underlying distribution. The statistics of the test were then averaged across the 100 simulations. Similarly, a 2-sample test for equality of



proportions was used to test whether damaged trees were different from standing trees in the type of trees in their  
145 surroundings (same species, different species with conifers or broadleaves).

## 2.2 Wind climate and models

A probability of wind damage can be calculated when combining calculated CWS from ForestGALES and information on extreme wind events. Three different descriptions of the wind climate were assessed in this study for their predictive power:  
150 the use of the maximum observed wind speed during the winter (October to April), the use of the Weibull distribution describing the mean wind climate assuming its convergence to a Gumbel distribution (as described in the ForestGALES default model), and the use of the Generalized Extreme Value (GEV) distribution describing the extreme – maximum wind speed climate.

### 2.2.1 Maximum observed wind speed during the winter 2020-2021

The maximum wind speed at 10m above ground was obtained from the hourly meteorological data from the long-term stable  
155 post-processed products of the Norwegian Meteorological Institute MET (available for download here: <https://thredds.met.no/thredds/metno.html>) on a 1 km x 1 km spatial grid across Norway. Since all damage was recorded during the winter of 2020-2021, corresponding to the period when tree falls occur most frequently in Norway, the search for the maximum observed wind speed was restricted between October 2020 and April 2021. The maximum wind speed for the winter 2020-2021 in the centroid of each of the 25 powerline strips and for each location of the 180 damaged trees was  
160 extracted. Some of the sites belonged to the same 1 km raster cell from the meteorological data, hence the final 2020-2021 maximum wind speed dataset contained 97 different locations for the 205 sites (25 powerline strips and 180 recorded individual tree damage events).

### 2.2.2 Weibull distribution – mean wind speed climate

The Global Wind Atlas (<https://globalwindatlas.info/en>) provides a worldwide description of the mean wind climate via the  
165 two Weibull distribution parameters A and k. Both parameters are available at a 250 m resolution (at the equator) and were downloaded for Norway. The value of the two parameters in the centroid of each of the 25 powerline strips and for each location of the 180 damaged trees were extracted. The maximum wind speeds described by a Weibull distribution converge to a Gumbel (GEV type I distribution – see below) distribution. The A and k parameters of the Weibull mean wind distribution can then be transformed into the two Gumbel parameters following Quine (2000) to describe the extreme wind  
170 climate based on information from the mean wind climate.

### 2.2.3 Generalized extreme value distribution – maximum wind speed climate

Since the extreme (maximum) wind speed climate is theoretically more relevant for assessing the probability of damage than the mean wind climate, it would be logical to use a model describing the extreme wind climate across Norway. Generalized



Extreme Value (GEV) distribution models are well-established and widely used in extreme value statistics (Palutikof et al., 175 1999). The GEV distribution was first introduced by (Jenkinson, 1955), describing three possible types of extreme value distributions for the block maxima of a given variable: type I – Gumbel, type II – Fréchet and type III – Weibull (Beirlant et al., 2004). The GEV distribution is a three-parameter distribution of the form:

$$G(X \leq x) = \begin{cases} e^{-[1+\xi \times (\frac{z-\mu}{\sigma})]^{\frac{1}{\xi}}}, & \text{for } \xi \neq 0 \\ e^{-e^{-\frac{z-\mu}{\sigma}}}, & \text{for } \xi = 0 \end{cases} \quad (1)$$

180 Where  $\mu$  is the location,  $\sigma$  is the scale, and  $\xi$  is the shape parameter. The shape parameter determines one of the three previously mentioned types: type I is when  $\xi = 0$ , type II is when  $\xi > 0$  and type III when  $\xi < 0$ . For an accurate parameter estimation of the GEV distribution at each site, the time series sample must be sufficiently long; a minimum of ten years of observations is recommended, but the longer the more accurate the estimates of wind extremes will be (Palutikof et al., 1999). There is however no published map of the three GEV parameters for Norway, therefore a GEV model was fitted on a 185 long-term dataset of yearly maximum wind speed for each of the sites. The long-term extreme wind speed dataset contained the yearly maximum wind speed for 47 years (1975-2021) extracted from the same data source as for the maximum wind speed observed in the winter 2020-2021 (i.e. the long-term stable post-processed products of the Norwegian Meteorological Institute MET). Similarly to this other dataset, it contained the time series of maximum wind speed for the 97 locations corresponding to the 205 sites.

190 For each of the 97 time-series, the GEV fitting procedure was as follows: (1) the Augmented Dickey-Fuller (ADF) and the Kwiatkowski-Phillips-Schmidt-Shin (KPSS) stationary tests were performed and stationarity of the time series was ensured (for  $\alpha = 0.05$ ); (2) the GEV distribution was fitted using the Maximum Likelihood Estimation (MLE); (3) each model fit was checked using two diagnostic plots: i) the empirical *versus* model quantiles plot with confidence bands, ii) the model density compared with the histogram of the empirical data; (4) both the Kolmogorov-Smirnov and Anderson-Darling tests were 195 performed to confirm the empirical data and a randomly generated sample from a GEV model with the estimated parameters originated from the same distribution. During step (2), initial estimates were supplied, in the form of the mean observed maximum wind speed across the time series for the location parameter, a scale value of 1 and a shape value of 0.1. The use of good initial estimates – especially for the location parameter – was important in ensuring convergence of the model. The final parameter estimates for the 97 fitted models were on average 10.5 (sd = 1.96) for the location parameter, 0.894 (sd = 200 0.241) for the scale parameter and -0.213 (sd = 0.130) for the shape parameter. The majority (94 out of 97) of the models showed a negative shape parameter, indicating a GEV model of type III. Traditionally, extreme wind speeds in temperate latitudes have been fitted to a Type I (Gumbel) distribution, as was done when using the Weibull distribution parameters in this study. However several published studies (Li et al., 2022; Palutikof et al., 1999; Soukissian and Tsalis, 2015) have shown that the Type III distribution is appropriate.

205 Note that the wind direction or seasonality of the extreme wind speed were not accounted for in this study.



## 2.3 ForestGALES, Critical Wind Speed and probability of damage

The ForestGALES model is a hybrid empirical and mechanistic wind risk model for forest stands and individual trees, initially developed in the United Kingdom (Hale et al., 2012, 2015) and now used in several European and non-European forest contexts (Duperat et al., 2021; Kamimura et al., 2016; Locatelli et al., 2016) and in Norway (Merlin et al., 2025). We 210 used the individual tree version (Turning Moment Coefficient – TMC – version). It uses input variables of tree characteristics, the surrounding forest stand, and soil class and rooting depth to calculate the Critical Wind Speed (CWS) for breaking and overturning damage. We used the R (*fgr*) package (Locatelli et al., 2022), which we recently parametrized for Norway (Merlin et al., 2025) and included an upgrade on crown asymmetry (details in section 2.2 and Appendix A).

### 2.3.1 Critical Wind Speed calculations

215 The CWS equations for breakage (Eq. (2)) and overturning (Eq. (3)) are shown below (Hale et al., 2015; Locatelli et al., 2022):

$$CWS_{breakage} = \sqrt{\frac{\pi \cdot MOR \cdot D_0^3 \cdot f_{knot}}{32 \cdot T_c \cdot TMC\_Ratio \cdot f_{Edge+Gap} \cdot DLF}} \quad (2)$$

$$CWS_{overturning} = \sqrt{\frac{C_{reg} \cdot W_{stem}}{T_c \cdot TMC\_Ratio \cdot f_{Edge+Gap} \cdot DLF}} \quad (3)$$

220 where  $\pi$ : pi mathematical constant;  $T_c$ : the turning moment coefficient (incorporating the effects of competition and very well correlated with tree size);  $D_0$ : diameter at base (derived from DBH; m),  $W_{stem}$ : stem weight (kg),  $MOR$ : modulus of rupture (MPa),  $MOE$ : modulus of elasticity (Pa),  $f_{knot}$ : species-specific factor accounting for the reduction in wood strength due to the presence of knots,  $f_{Edge+Gap}$ : the combined effect of the tree position relative to the upwind stand edge and the size of the upwind gap,  $DLF$ : deflection loading factor accounting for the added bending moment due to the displaced crown and stem (Locatelli et al., 2022),  $C_{reg}$ : species-specific overturning coefficient empirically describing the root anchorage for different soil and rooting depth combinations (Nm/kg) (Nicoll et al., 2006). See Hale et al. (2012, 2015) and Locatelli et al. 225 (2022) among others for more in-depth information and definitions of the different parts of the ForestGALES model for the individual tree version.

230 The CWS for damage – the minimum between the CWS for breakage and overturning – was calculated for each tree under three different seasonal scenarios:

- A “summer” scenario, where birch trees have a full crown and without any snow loading
- A “fall” scenario, where birch trees have lost their leaves without any snow loading



235 - A “winter” scenario, where birch trees are without leaves and tree crowns of all tree species are loaded with the local (1 km resolution) maximum snow load for the winter 2020-2021. Briefly, the maximum snow load on individual tree crowns for the winter 2020-2021 was extracted from the 2013-2023 timeseries of hourly crown snow load calculated following Lehtonen et al. (2014) on the climate data from the same long-term stable post-processed products of the Norwegian Meteorological Institute MET. Note that this method does not account for species’ differences in crown shape and probably overestimates crown snow load for birch trees. The frequency distribution 240 of the crown snow load values for the 2020-2021 winter for the 97 MET locations (corresponding to the 205 sites) is shown in Appendix A Fig. A1.

### 2.3.2 Probability of damage

245 The CWS values on their own offer a broad view into which trees are structurally more vulnerable to damage than others, but this does not account for the wind climate of the area. The probability of damage can be calculated in different ways depending on the wind data and model(s) available and chosen. In this study, we tested three methods based on the probability of exceeding the CWS:

- Using a logistic function (Gardiner et al., 2024): the maximum wind speed observed during the actual winter 2020-2021 ( $ws_{20.21}$ ) at each location was compared with the calculated CWS. The wind speed was either kept as is or further adjusted by the local  $Topex$  value. The equation for predicting the probability of damage is below:

$$250 \quad Prob_{WS2021} = \frac{1}{1 + exp\left(-\frac{\left(ws_{20.21} \times \left(1 - \frac{Topex}{Topex_{max}}\right)\right) - CWS}{S}\right)} - \frac{1}{1 + exp\left(\frac{CWS}{S}\right)} \quad (4)$$

The factor S is a slope factor, and set to 6 as in (Chen et al., 2018; Gardiner et al., 2024). The value  $Topex_{max}$  is taken as the maximum  $Topex$  value across all considered locations and for the horizon chosen (i.e. 200, 500 or 1000 m).

255 - Using the annual probability of damage using a 30-year time period of wind data and a Generalized Extreme Value Distribution model describing the maximum wind climate at each location. The probability of damage can therefore be calculated as:  $Prob_{GEV} = 1 - G(X \leq CWS)$  where  $G(X \leq x)$  is defined in Eq. (1).

- Using the annual exceedance probability function default in the ForestGALES model and fgr package. Using the Weibull A and k parameters describing the mean wind climate, the probability of exceeding the CWS is given using the Fischer-Tippett (i.e. GEV) Type I distribution since the extremes of a dataset following a Weibull distribution 260 (the mean hourly wind speeds) converge towards a Gumbel (GEV type I) distribution. The probability of damage is



then given by the function for the annual exceedance probability in fgr (which is a slightly modified type I GEV from Eq. (1)):

$$\begin{cases} U = [A \times (c_1 \times k^3 + c_2 \times k^2 + c_3 \times k + c_4)]^2 \\ Prob_{Weib} = 1 - \exp \left( -\exp \left( \frac{-(CWS^2 - U)}{U/5} \right) \right) \end{cases} \quad (5)$$

265

Where the parameters  $c_i$  for  $i \in \{1:5\}$  are constants and equal to (Quine, 2000):

$$c_1 = -0.5903; c_2 = 4.4345; c_3 = -11.8633; c_4 = -13.569.$$

## 2.4 Validation

In total, we considered the damage predictions from several models covering the different definitions of tree characteristics, 270 seasonal scenarios, forest gap and edge definition and method for calculating the probability of damage (Fig. 2).

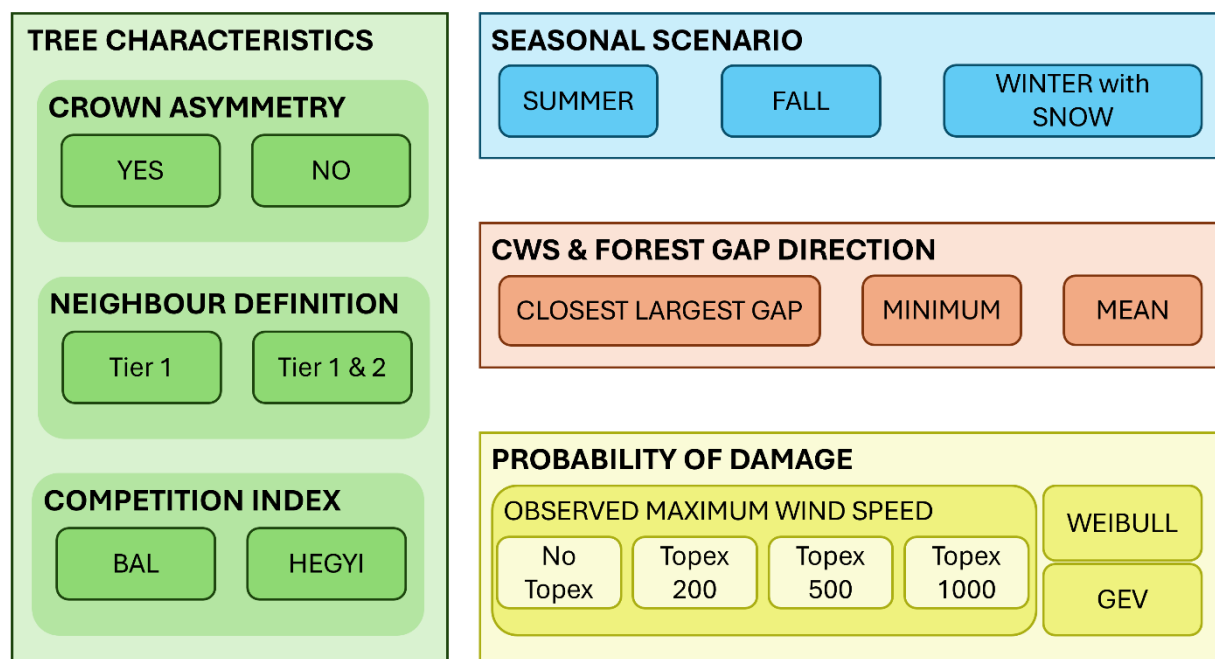


**Figure 2.** Summary of all the model options considered in the study when assessing the performance of the individual tree predictions for damage using the ForestGALES model – across tree characteristics (in green), the seasonal scenario considered (in blue), the calculation of the Critical Wind Speed (CWS) in relation to the forest gap direction considered (in orange) and the wind data and probability function used for calculating damage. The “closest largest gap” was defined using the linear optimizer function of the lpSolve package in R (Berkelaar, 2024), while the “minimum” was simply the closest gap and “mean” the average of the distances to and size of the non-forested gaps in the four considered directions (to and from the powerline, and along the powerline direction).

We confronted the damage probability predictions to the observed damage for all models considered. We created contingency tables identifying the true positives (TP), true negatives (TN) and false positives and negatives (FP and FN) for

275



280 a probability cutpoint varying from 0 to 1 with a step of 0.1. The cutpoint was used to convert the continuous damage  
probability to a binary prediction of Damage/Standing. We then calculated the sensitivity ( $TP/(TP+FN)$ ) and specificity  
( $TN/(TN+FP)$ ) of the models and ranked the discrimination power of the models using the AUC (Area under the curve) of  
the Receiver Operating Characteristic (ROC). The AUC is commonly used to summarize the accuracy of the model, taking  
values between 0 and 1. In general, an AUC value of 0.5 suggests no discrimination – the model discrimination ability is no  
285 different from random – while values between 0.7 and 0.8 indicate acceptable discrimination, between 0.8 and 0.9 is  
considered excellent and above 0.9 outstanding (Hosmer et al., 2013).  
Given that the data is unbalanced in terms of the ratio of damaged/standing trees as described in section 2.1.3, the assessment  
of the models' performance (AUC from the ROC) was done on 100 repetitions of balanced damaged/undamaged ( $N = 180$   
for each) datasets. The final AUC value for each of the tested models was the average of the AUC from the 100 repeated  
290 assessments.

## 2.5 Machine learning for improving discrimination

### 2.5.1 Choice of the eXtreme Gradient Boost machine learning algorithm

Machine learning (ML) methods can provide a complementary approach to mechanistic models such as ForestGALES. The  
ML models are purely data-driven and can provide predictive power based on complex multivariate relationships that may  
295 not be captured in the models or not yet discovered. By combining ForestGALES with an ML model on a multivariate dataset,  
the calculated CWS and characteristics from the wind climate and landscape exposure to wind may prove to generate better  
predictions of individual tree fall (Hart et al., 2019). Moreover, ML models can be used as proxy models, approximating the  
behaviour of a mechanistic model while speeding up the computation time. An ML surrogate using all tree, soil, landscape  
and wind data bypassing the calculation of CWS could provide a quicker wind risk assessment in decision-support systems  
300 for individual tree management for forest stakeholders (e.g. powerline and railway companies). The training of ML  
algorithms requires however large datasets. The sample of 180 damaged trees in this study is at the low end of sample sizes  
for fitting ML algorithms. We explored this method nonetheless to assess its potential and set up a precedent for future  
studies combining ML and ForestGALES. For this reason, no distinction was made between species when running the ML  
algorithms; only the best global model previously selected was used in determining the CWS used in the input dataset for the  
305 ML algorithm.

The ML algorithm used in this study was the eXtreme Gradient Boosting algorithm (XGBoost), an efficient and reliable  
method for regression and classification (Chen and Guestrin, 2016). The algorithm is a tree-based incremental learning  
process. At each iteration, a new weak learner is trained based on the error of the decision tree previously learned. Gradient  
boosting iteratively adjusts the predictions of the decision trees by minimizing the loss function (based on the error between  
310 the predicted and observed values), splitting and removing less significant tree nodes. Then, all decision trees are combined,  
and the predictions from each tree are weighted based on their importance. The iterative process is repeated until either a



specific number of iterations are completed, or a predefined criterion is met. Many of the hyperparameters of the XGBoost algorithm can be modified and tuned. To keep it simple, we did not tune the hyperparameters and we used a set of default hyperparameters following the documentation of the *xgboost* R package. The values used for the main hyperparameters of  
315 the XGBoost algorithm are summarised in the Appendix A Table A2.

### 2.5.2 Input datasets to the XGBoost algorithm

Two types of datasets were used in the XGBoost algorithm. The first dataset – hereafter referred to as the “ForestGALES-ML” dataset – contained the individual tree CWS value calculated by ForestGALES, the exposure index Topex at 200 m, and a variable describing the local wind climate: either the maximum observed wind speed during the winter 2020-2021  
320 (“max\_ws”), the 1-year return level (*i.e.* the location parameter) of either the GEV model (“return\_gev”) or the Weibull model (“return\_weib”). By using this first dataset, we assessed the potential in combining a mechanistic model (ForestGALES) to obtain a vulnerability index (CWS) and then a ML algorithm to obtain better damage predictions. The second dataset – hereafter referred to as the “TreeChar-ML” dataset – contained the same individual tree information used as input to the ForestGALES model (tree height, DBH, crown width and depth, crown offset, stand mean DBH, crown width  
325 and depth, and stand top height) as well as the ForestGALES soil and rooting depth classes, the exposure index Topex at 200 m and one of the three available variables describing the local wind as in the “ForestGALES-ML” dataset.

### 2.5.3 Training of the XGBoost algorithm and assessment

We trained the XGBoost algorithm in the same way for both datasets. The input dataset was biased towards a uniform class distribution as described in section 2.5, selecting an equal number of damaged and standing trees, N=180, 100 times. For  
330 each of the 100 datasets, the XGBoost algorithm was trained and tested using a 10-folds cross-validation procedure. The data was randomly partitioned into 10 subsamples (folds) of equal size. Nine folds are combined to train the algorithm, and the last fold is used to test the algorithm. The procedure was repeated by leaving out each of the 10 folds in turn. The AUC value, accuracy and feature (variable) importance (measured with the gain – the fractional contribution of each variable to  
335 the model) were measured as the mean from their respective values for each of the 10 repetitions from the cross-validation procedure. The AUC, accuracy and feature importance reported hereafter are their mean (and standard deviation “sd”) values across the 100 repetitions.

The XGBoost algorithm returned a probability of damage. The discrimination threshold between damaged and standing trees used was 0.5, such that a probability equal or greater than 0.5 resulted in the damaged classification.

## 2.6 Software

340 We accessed and processed the meteorological data using GDAL/OGR 3.4.3 (Rouault et al., 2022), and CDO version 1.9.9rc1 (Climate Data Operators, <https://mpimet.mpg.de/cdo>). All analyses were done using the statistical software R 4.3.3 (R Core Team, 2024). The GEV model fitting was performed with the *extRemes* package (Gilleland and Katz, 2016). The *fgr*



R library (Locatelli et al., 2022) and its extension in a C++ version (Merlin et al., 2025) implemented in R with the *Rcpp* package version 1.0.11 (Eddelbuettel et al., 2023) were used to calculate the individual CWSs. The XGBoost algorithm was 345 fitted with the *xgboost* package (Chen et al., 2024). Maps were generated using the *terra* and *tidyterra* packages (Hernangómez, 2023; Hijmans, 2024) and all other figures with the packages *ggplot2* and *ggpubr* (Kassambara, 2023; Wickham, 2016).

### 3 Results

#### 3.1 Characteristics of damaged and undamaged trees

350 Basic information on the tree height and DBH of the damaged *versus* standing trees is presented in Table 1. The damaged trees tended to be smaller in both height and diameter than the standing trees, whether considering all species together or individually. No significant difference in the H/d ratio was found between the damaged and standing trees for any of the three species. The damaged trees were typically not the tallest trees in their surroundings and were similar to the standing trees in their relative height to the surroundings' top tree. The damaged trees tended to have a smaller ratio of crown depth to 355 tree height (meaning that they had a shorter crown for a given height) than the standing trees, but this result was mostly driven by Scots pine and birch trees to a lesser extent (results not shown). There was no difference in the tree type (same species, different species and conifer or different species and broadleaf) of the surrounding trees between damaged and standing trees.

360 **Table 1.** Mean (standard deviation) values statistics between the damaged and undamaged (standing) trees for tree height (in meters), tree DBH (in centimetres), the ratio of tree height to DBH ("d/H ratio") between the damaged and undamaged (standing) trees. The U statistic (Mann-Whitney-Wilcoxon test) are shown, along with the p-value associated with those statistics. \*, p < 0.05; \*\*, p < 0.01; \*\*\*, p < 0.001, ns: not significant ( p > 0.05).

Variable	Species	Damaged	Standing	U value	p-value	Comment
Tree height	all	14.05 (5.09)	18.36 (4.79)	8803.6	***	Damaged trees are smaller
	Birch	13.89 (5.07)	18.77 (4.44)	844.2	***	
	Norway spruce	15.85 (5.39)	18.41 (4.88)	1519.4	*	
	Scots pine	12.62 (4.25)	17.95 (5.01)	580.1	***	
Tree DBH	all	20.93 (9.96)	27.23 (11.56)	8940.3	*	Damaged trees are thinner
	Birch	20.79 (13.15)	31.12 (17.87)	792.3	*	
	Norway spruce	18.58 (5.09)	21.74 (4.72)	1338.7	**	
	Scots pine	23.33 (6.52)	31.35 (7.74)	579.6	***	
H/d ratio	all	0.71 (0.17)	0.69 (0.16)	15375	ns	No difference
	Birch	0.66 (0.12)	0.69 (0.15)	2027.1	ns	
	Norway spruce	0.84 (0.12)	0.84 (0.11)	1952.6	ns	
	Scots pine	0.58 (0.11)	0.54 (0.09)	1011.4	ns	



### 3.2 Damage probability during the winter 2020-2021

#### 3.2.1 Performance of all tested models

365 Several options were tested for calculating the CWS and probability of damage: the use of a crown offset, neighbour level, competition index, seasonal scenarios, type of CWS in terms of gap and edge definition, wind data/model type and the use of multipliers for CWS and the wind speeds (summarized in Fig. 2). All models were assessed for their discrimination power – defined by the AUC – based on the calculated probability of damage using 100 repeated assessments with a balanced sample of damaged and standing trees (see Sect. 2.5). Only 20% (global models) and 23% (species-specific models) of all tested  
370 models yielded an AUC above 0.6. The mean AUC across the different alternatives for all the tested models an AUC above 0.6 are presented in Appendix B Fig. B1. Among the models with an AUC above 0.6, the models with the BAL competition index significantly outperformed the alternative for the global and species-specific models except for Norway spruce. The models using the tier 1 & tier 2 or tier 2 neighbour levels had higher AUC values than the alternative neighbour level. There were no clear differences in performance among the alternatives for the inclusion of the crown offset and CWS type across  
375 all the tested global and the species-specific models. The different seasonal scenarios performed similarly for the global models, but the AUC values for the winter scenario were lower for birch (significant difference) and Norway spruce (non-significant difference) and higher for Scots pine than the fall and summer scenarios. Surprisingly, the use of the GEV wind model performed the worst: only 9% of all models using the GEV wind model yielded an AUC value above 0.6. Despite representing the extreme wind climate at each location, it performed worse than the Weibull model which described the  
380 mean wind climate (Appendix B Fig. B2). Using a logistic probability function with the actual observed maximum wind speed for the winter 2020-2021 (“Actual WS”, Eq. (4)) yielded the highest AUC across the different wind data/model options for the global and species-specific models except for Norway spruce where the use of the Weibull model outperformed it (by 0.05 AUC units, Appendix B Fig. B2). Overall, including a Topex correction did not improve the performance of the models under the “Actual WS” alternative (Appendix B Fig. B2).

385 **3.2.2 Best global and species-specific models**

The best global and species-specific models – the ones achieving the highest AUC values under the 100 repeated simulations – were selected and presented in Table 2. None of the global models achieved an AUC value above 0.7. The best global model yielded an AUC of 0.676. The best species-specific models all achieved AUC values at or above 0.7. The cutpoint (for converting the damage probability predictions to binary Damaged/Standing predictions) was generally quite low across  
390 the selected best global and species-specific models, indicating that the ForestGALES model overestimates the CWS, therefore overestimating of the damage probability.

**Table 2.** Description and performance assessment of the best models for predicting the observed tree damages during the winter 2020-2021. The best models across species (“All”) and for each of the species were the models which yielded the highest AUC values across the 100 repeated assessments of model performance using a balanced sample of damaged and standing trees. When the symbol “-” is used for one of the model options, this indicates that all of the option’s alternatives yielded a similar AUC value. Accuracy of the model is  
395



calculated where the cutpoint gives equal model Sensitivity and Specificity. CLG: Critical Wind Speed from the closest largest gap when available.

		Global model	Species-specific models		
			Birch	Norway spruce	Scots pine
	<b>Seasonal scenario</b>	Winter	Fall	Fall	Winter
	<b>Competition index</b>	BAL	BAL	BAL	BAL
	<b>Crown offset</b>	no	no	yes	yes
<b>Model options</b>	<b>Neighbour level</b>	tier 1 & tier 2	tier 1 & tier 2	tier 1 & tier 2	tier 1 & tier 2
	<b>CWS type</b>	-	CLG	CWS <sub>min</sub>	CWS <sub>min</sub> - Actual wind speed
	<b>Wind data</b>	Actual wind speed	Actual wind speed	Weibull model	
<b>Model performance</b>	<b>AUC</b>	0.676	0.727	0.698	0.734
	<b>Accuracy (%)</b>	62.2	62.5	68.4	62.5
	<b>Cutpoint</b>	0.221	0.191	8 10 <sup>-5</sup>	0.216

The ROC curve for the best global and species-specific models selected is presented in Figure 3, using all samples. The overall accuracy of the best global and species-specific models was ~64%, meaning that about 64% of the damaged and

400 standing trees were correctly identified by the models.

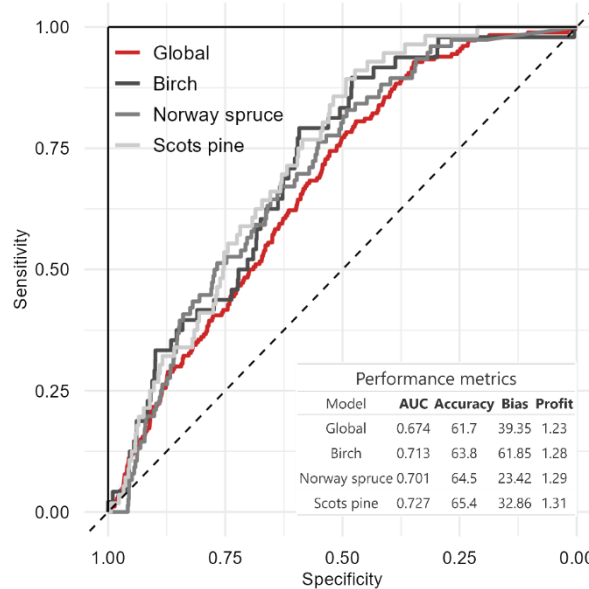


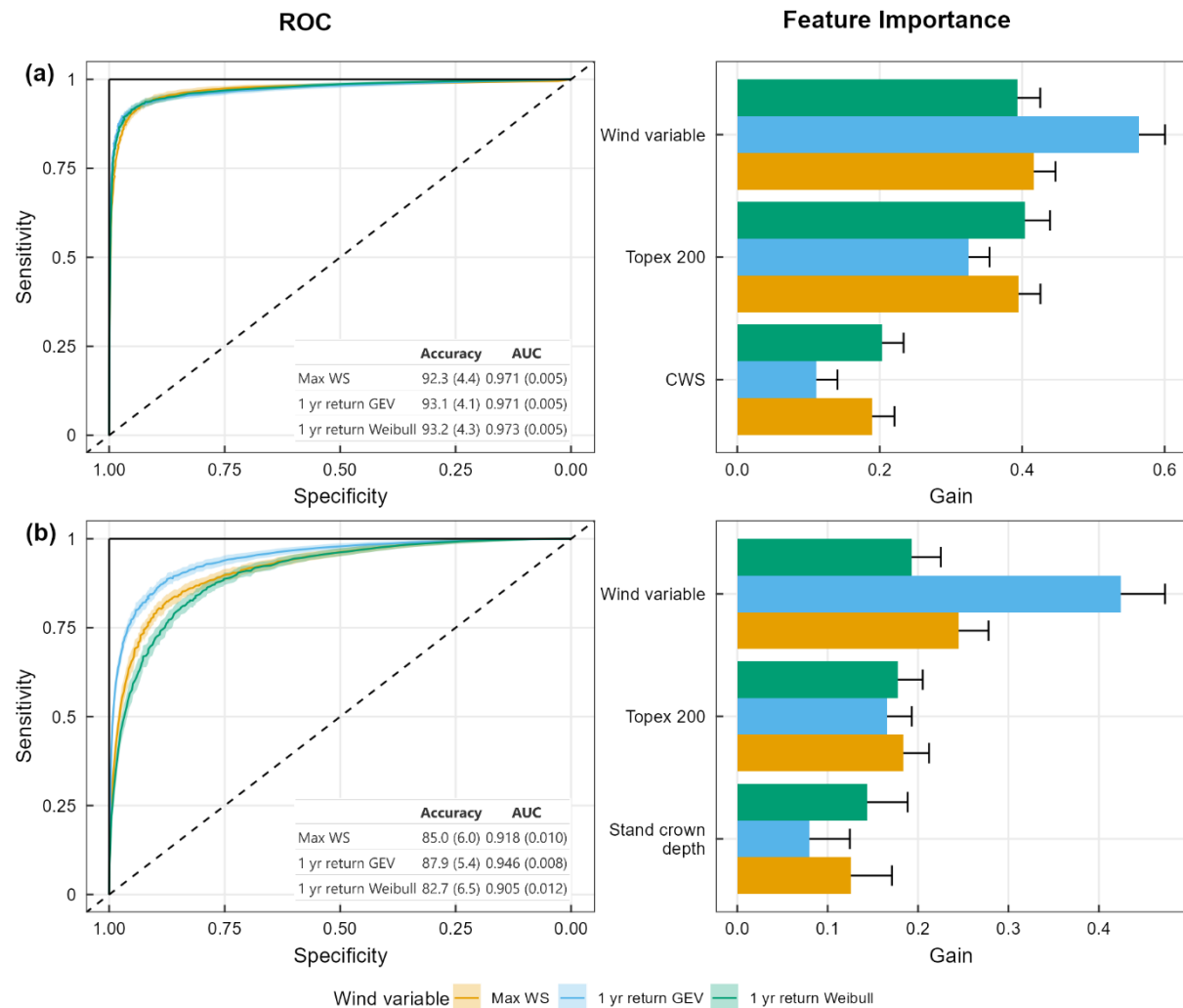
**Figure 3.** Receiver Operator Characteristic (ROC) curve and performance metrics for the prediction of the probability of tree damage during the winter 2020-2021 using the best global and species-specific model options (see Table 2). All samples were used in this figure ( $N_{\text{damaged}} = 180$ ;  $N_{\text{standing}} = 18,189$ ). The AUC is shown in the table, along with the summary of the performance metrics (Accuracy in percentage, Bias, and Profit scores) for the cutpoint at which Sensitivity = Specificity.

### 3.3 Improved damaged predictions with machine learning

A simple implementation of an extreme gradient boosting algorithm was used to improve the predictions of individual tree damage, building on the selected best global model previously identified. The XGBoost algorithm output a probability of damage, which was then transformed into a binary prediction of Damaged/Standing using an arbitrary threshold of 0.5. The



410 algorithm yielded outstanding classification results with both the “ForestGALES-ML” and “TreeChar” datasets, with a mean AUC of or above 0.9 for all three wind variables used across the 100 repetitions. The results with the ForestGALES-ML dataset slightly outperformed the ones with the TreeChar-ML dataset (Fig. 4).



415 **Figure 4.** Summary of the XGBoost algorithms performance (ROC curve; left) and feature importance for the top three contributing variables (right) when using the “ForestGALES-ML” dataset (panels a) and the “TreeChar-ML” dataset (panels b) for the 100 repetitions across the three alternatives for the wind variables. The three alternatives are: Max WS (in orange), the 1-yr return GEV (blue) and the 1-yr return Weibull (green). The mean (and sd) AUC and accuracy across the 100 repetitions of the 10-folds cross-validation procedure for each alternative of the wind variables are shown as a table in the two left panels.

420 Across both the “ForestGALES-ML” and “TreeChar” datasets, the wind variable and Topex at 200 m were the two variables with the highest mean gain (Fig. 4). The CWS came in third and last for the XGBoost algorithm applied to the “ForestGALES-ML” dataset, while a mix of stand and tree variables shared the lower ranks of feature importance for the “TreeChar-ML” dataset (see the Appendix B Table B4 for the full list and feature importance metrics for both datasets).



Considering the large importance of the Topex200 variable in the XGBoost algorithms, we removed it and ran the XGBoost algorithms on both datasets once more to assess the ability of the ML algorithm to predict wind damage without this  
425 variable. The removal of Topex200 slightly accentuated the differences in performance between the three alternative wind variables used in the XGBoost algorithms. For both datasets, the use of the 1-yr return GEV outperformed the other two alternatives (results not shown). On average, the removal of Topex200 decreased the mean AUC by 0.04 points for both the ForestGALES-ML and TreeChar-ML datasets. Similarly, the accuracy dropped by an average of 4% across the three  
430 alternative wind variables. The wind variable was then further removed from the XGBoost algorithm input for the TreeChar-ML dataset to assess its performance when considering only tree characteristics variables. The AUC was then significantly reduced, down to 0.763 for an accuracy of ~70%.

## 4 Discussion

This study used the hybrid mechanistic wind risk model ForestGALES to predict individual tree fall during winter 2020-2021 along powerline strips in southern and western Norway. This is the first study using ForestGALES at the individual  
435 tree level considering both wind and snow load in predicting tree fall. The model performed reasonably well. Its performance varied across species, and across how tree characteristics, environment and the probability of damage were defined. The machine learning results performed excellently and painted the familiar picture of Risk = Vulnerability x Exposure. It highlights the importance of the background wind, local shelter modulating the background wind in the landscape, and by tree vulnerability when predicting wind damage. These results reaffirm the potential of using ForestGALES operationally in  
440 designing precision vegetation management along linear infrastructure (Gardiner et al., 2024).

### 4.1 Remote sensing methods for mapping vulnerable trees along linear infrastructures

Remote sensing techniques have proven invaluable both for informing precision forest management and rapid damage assessment. Precise and individual tree-based vegetation management along linear infrastructures requires detailed data at the individual tree level (Sey et al., 2023). Here, the UAV-LS method provided accurate positioning of individual trees along  
445 powerlines and in their immediate environment. It allowed for a better characterization of the individual tree crown characteristics important in the calculation of the CWS. The use of a higher point cloud density in the UAV-LS system could provide a direct estimation of the trees' diameter and crown length (Straker et al., 2023), two critical variables in the CWS calculation (Locatelli et al., 2017). This however comes at a higher cost and a more intensive post-processing task, which may be impractical for operational vegetation management currently. After a storm event, remote sensing can quickly, efficiently and safely map windblown trees, especially in complex and difficult terrain (Dalponte et al., 2020; Reder et al.,  
450 2025). This is critical for a rapid assessment of the damage for forest owners, managers, insurance companies and other institutions but also may provide a rapid expansion of available damaged datasets to test and validate models such as ForestGALES. Validation data remain scarce for storm events especially in complex landscapes such as in Norway, and



when the threat of secondary mortality from insects and pathogens benefitting from windblown trees (e.g. spruce bark beetle  
455 in spruce-dominated stands) requires rapid salvage logging operations. Remote sensing methods can be deployed quickly  
and contribute to filling this data gap.

#### 4.2 Fair performance of ForestGALES in identifying vulnerable trees

Compared to the traditionally used H/d ratio which showed no difference between damaged and standing trees here, the  
460 performance of ForestGALES in identifying vulnerable trees was adequate across all model specifications considered (see  
Figure 2). In general, the differences in AUC across all the model specifications were rather small, on average less than 0.05  
points in AUC (Appendix B Fig. B2) but up to 0.2 points for the wind data type used (Appendix B Fig. B3). Not all model  
specifications performed similarly across the three tree species – e.g. the conifer models showed improved performance  
when accounting for the crown offset but not the birch model nor the global model. This may stem from species differences  
465 in the role of the different variables in the determination of their vulnerability against wind – the example of the crown offset  
may come from the difference in crown shape and contribution to wind vulnerability between the tree species considered, from  
unexplained bias in the dataset emerging in the results (e.g. the better performance of the Weibull model for the  
Norway spruce model) or from the rather simple crown shape used in ForestGALES. In summary, the best model across  
species for predicting damage in the winter 2020-2021 season considered the addition of crown snow load, with a basal-area  
based competition index between trees (BAL) but without considering the crown offset, accounting for the larger immediate  
470 environment (tier 1 & tier 2 neighbour level) and using the actual observed wind speed for the calculation of the probability  
of damage.

The middling performance of ForestGALES highlights some of this study's limitation and opportunities for future work. The  
475 discrimination between standing and damaged trees was adequate but failed to reach the commonly accepted threshold of 0.7  
of good discrimination power across almost all the tested models. ForestGALES was soft-parametrized for the Norwegian  
forest conditions (from Merlin et al. (2025)) therefore may fail to capture local and more complex variations in wood, root  
anchorage properties, and crown structure observed across the study area. Statistical parametrization and further  
development to the model could be considered (Lorenz et al., 2024; Stadelmann et al., 2025) but requires extensive damaged  
datasets. In general, the model's damage predictions were too conservative – as seen with the rather low cutpoint for damage  
in the ROC analysis (Table 2). Overestimation of the critical wind speed may stem from unaccounted factors at the tree level  
480 such as tree age and health. Importantly, decay and root rot caused by *Heterobasidion* sp. in Norwegian forests and more  
specifically in spruce-dominated forests – is a major disturbance agent which targets the root system and progresses up the  
stem, significantly weakening the anchorage and resistance of the tree against wind (Krisans et al., 2020; Žemaitis et al., 2024).  
This is also the first time the snow load module of ForestGALES was used in assessing wind damage risk at the individual  
tree level. The snow module has yet to be validated in the field and uncertainties around the crown snow load calculations  
485 can further bias the estimate of CWS under snow load. Note that a derivation of this snow module in ForestGALES was used  
and successfully tested in (Zubkov et al., 2024). However, this study's results are the first step towards validation, and brings



forth the importance of seasonal conditions when considering wind damage in trees. Beyond the CWS estimation, we've seen that the type of wind data used influences the results. The choice between using the mean maximum historically observed wind speed, Weibull model parameters of mean wind climate or the extreme value model for extreme wind climate 490 should be made according to the scenario in line with this study. No extreme wind speeds were observed during the 2020-2021 winter season – hence the relatively poor performance of the GEV models. We are also operating at the limit the ForestGALES model, developed for estimating damage vulnerability during storm events, and had a limited number of damaged trees. Therefore, we cannot exclude that some of the recorded tree falls may have occurred due to other factors than wind (for example root rot damage for Norway spruce trees).

#### 495 **4.3 Improving damage predictions with Machine Learning**

Combining machine learning algorithms with the vulnerability index from ForestGALES significantly improved the damage predictions at the individual tree level. The machine learning model applied solely to the tree characteristics dataset (called “TreeChar-ML” in this study) showed much better performance than the ForestGALES model alone. More importantly, the machine learning model integrating the CWS as one of the predictors performed even better. It highlights 500 the possibility to rely on both our understanding of the mechanics of wind damage on trees and forests with machine learning for accounting for yet unknown factors or processes that affect the risk of damage. Several recent studies have already seen the potential for machine learning to identify trees vulnerable to wind damage (Jahani and Saffariha, 2022; Morimoto et al., 2021; Pawlik and Harrison, 2022). Combined with remotely sensed data, it can provide a powerful tool to accurately map scattered and sparse damage areas in complex terrain to manage efficient and safe salvage logging operations. Nonetheless, 505 one critical aspect of using machine learning models is their reliance on large input datasets. The performance of ML algorithms and their subsequent use depends on the quantity and quality of the data supplied to train the models, which can be limited in the case of forest ecology (Liu et al., 2018) and even more for scattered forest damage. Our study had a very limited number of fallen trees ( $N = 180$ ), nearing the lower limit for applying ML algorithms thus interpretation should be made cautiously. An effort to routinely collect comprehensive wind-driven damage data should be a priority to improve the 510 ML algorithm training, necessary for using the model for damage predictions in other locations in Norway.

#### **4.4 Risk mapping for single-tree management along linear infrastructures**

The identification of vulnerable sections based on individual tree surveys could be the most practical goal for implementing a routine vulnerability assessment in vegetation management plans along linear infrastructures. Our study and a previous 515 study along railway lines in Germany (Gardiner et al., 2024) showed that prediction at the individual tree level using ForestGALES alone is adequate or even good. In practice, utilities and other companies or institutions managing linear infrastructures are unlikely to design management plans based on individual tree predictions. Rather, the identification of vulnerable or priority sections can provide a solution mitigating costs while targeting vulnerability issues and designing smart vegetation management plans. The calculation of the CWS with ForestGALES (or a similar damage threshold index)



at the individual tree level could be translated into vulnerability along forest sections and integrated in the management  
520 assessment process. Unfortunately, this option could not be investigated in this study due to the sampling design. It can be tied together with modules exploring economic consequences and scenario preparation, finally assigning a wind and economic vulnerability score later used in drafting vegetation management plans. The powerline companies have a strong interest in developing and implementing such processes – from remotely sensed individual tree data to a vulnerability score along forest sections to prioritise their management efforts and reduce damage risks.  
525 Routes for the new linear infrastructures could therefore be evaluated in terms of potential wind damage risk with ForestGALES, along with other measures of impacts (biodiversity, timber production, slope stability etc...) using remote sensing for surveying the available landscape or with existing high-resolution forest resource maps. Such a comprehensive assessment can help balancing risk mitigation with provisioning of ecosystem services and minimize the footprint of linear infrastructures expansion in forests (Dupras et al., 2016; Garfinkel et al., 2023). Different management strategies can also be  
530 explored for these new routes but also for existing routes when combining ForestGALES with forest stand and tree dynamics models over time, thereby informing the managers of the range of options, trade-offs and potential feedbacks that different management options offer (Öhman et al., 2025).

## 5 Conclusions

Mathematical modelling based on high-resolution remote sensing data has a potential for estimating the probability of wind-  
535 throw for individual trees along linear infrastructures under different seasonal and climate scenarios. The ForestGALES model performed adequately, while an extension of this into an ML approach performed better. We believe this represents a possible support for managing trees along linear infrastructures in the forest. It can be integrated in a process evaluating and optimizing different vegetation management strategies to balance economic and safety aspects, wind risk, and other forest ecosystem services.



## 540 Appendices

### Appendix A Supplementary Methods

#### A.1 Processing of the individual tree dataset

##### A.1.1 Species specific equations for estimating diameter at breast height

545 **Table A3.** Species-specific dendrometric equations for estimating diameter at breast height (DBH, cm) from UAV-LS (unmanned aerial vehicle – drone – Laser scanning) derived mean height and crown dimensions (area and diameter) based on a field survey conducted by eSmart Systems in summer 2021.

Species	Equation	N	R <sup>2</sup>
Norway spruce	$DBH_{spruce} = (2.40343 + 0.07609 \times height + 0.35885 \times crown_{diameter})^2$	74	0.67
Scots pine	$DBH_{pine} = (2.679883 + 0.117317 \times height + 0.088388 \times crown_{area} - 0.001929 \times crown_{area}^2)^2$	71	0.43
Broadleaves	$DBH_{broadleaves} = \exp(1.988877 + 0.048793 \times height + 0.025854 \times crown_{area})$	32	0.74

##### A.1.2 Displacement of the crown centre of gravity under asymmetry

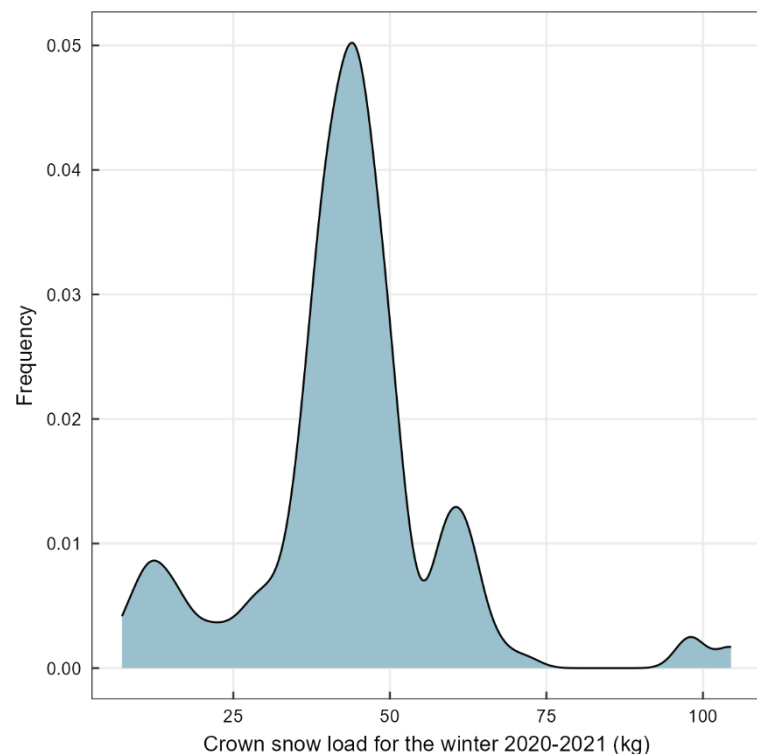
550 A measure of the crown asymmetry for each tree was done using the 8 crown radii available in the single tree dataset. We estimated the displacement of the centre of gravity between a right circular cone shape and an irregular cone. The centre of mass is assumed to be at ¼ height of the crown depth above the crown base under both scenarios. The calculation went as follows: first each of the 8 radii and their direction (expressed as an angle from 0 to 315 degrees) were positioned on the xy plane (centred on the positioning of the top of the tree) (Eq. (A1a)) where  $i$  is one of the 8 cardinal directions. Second, the position  $(x_g; y_g)$  of the centre of gravity was calculated as the mean of the 8 pairs  $(x_i; y_i)$  (Eq. (A1b)). Finally, the crown asymmetry was calculated as the distance between the theoretical crown centre of gravity – taken as the position of the top of 555 the tree, i.e. the origin of the xy plane – and the calculated new position of the centre of gravity (Eq. (A1c)).

$$\left\{ \begin{array}{l} x_i = radius_i \cdot \cos(angle_i); y_i = radius_i \cdot \sin(angle_i), \quad (a) \\ x_g = \bar{x}_i; y_g = \bar{y}_i, \quad (b) \\ crown\ offset = \sqrt{x_g^2 + y_g^2}, \quad (c) \end{array} \right.$$

(A1)



## A.2 Maximum crown snow load for the winter 2020-2021



560 **Figure A5.** Frequency distribution of the maximum calculated crown snow load (kg) for the winter 2020-2021 for the 25 individual powerline strips and 180 recorded damaged trees. Briefly, crown snow load was calculated hourly for the 2013-2023 timeseries using (Lehtonen et al., 2014) on the hourly meteorological data from the long-term stable post-processed products of the Norwegian Meteorological Institute MET (<https://thredds.met.no/thredds/metno.html>) at a 1km resolution. The maximum for the winter season 2020-2021 was then extracted for the grid cells corresponding to each of the 205 locations (25 powerline strips and 180 fallen trees).

565 **A.3 Machine Learning parameters**

**Table A4.** Description and value of the main hyperparameters used for the XGBoost (eXtreme Gradient Boosting) algorithm with a 10-fold cross-validation procedure.

Hyperparameter	Description	Value
eta	step size shrinkage of the weights associated with features used to prevent overfitting after each round	0.3
gamma	specifies the minimum loss reduction required to make a split – the larger gamma is the more conservative the algorithm is	0
max.depth	maximum depth (number of nodes) of a tree	3 for the ForestGALES_ML dataset; 6 otherwise
subsample	fraction of observations used to train individual trees – controls the randomisation of the algorithm	1
colsample_bytree	fraction of features used to train individual trees – controls the randomisation of the algorithm	1
min_child_weight	minimum weight required to create a new node in the tree	1
nrounds	maximum number of iterations	500



---

objective	learning objective of the algorithm – here logistic regression for binary classification, with a probability as output.	binary:logisitc
metrics	evaluation metric to be used in the cross-validation procedure – here the binary classification rate	error

---



## Appendix B Supplementary Results

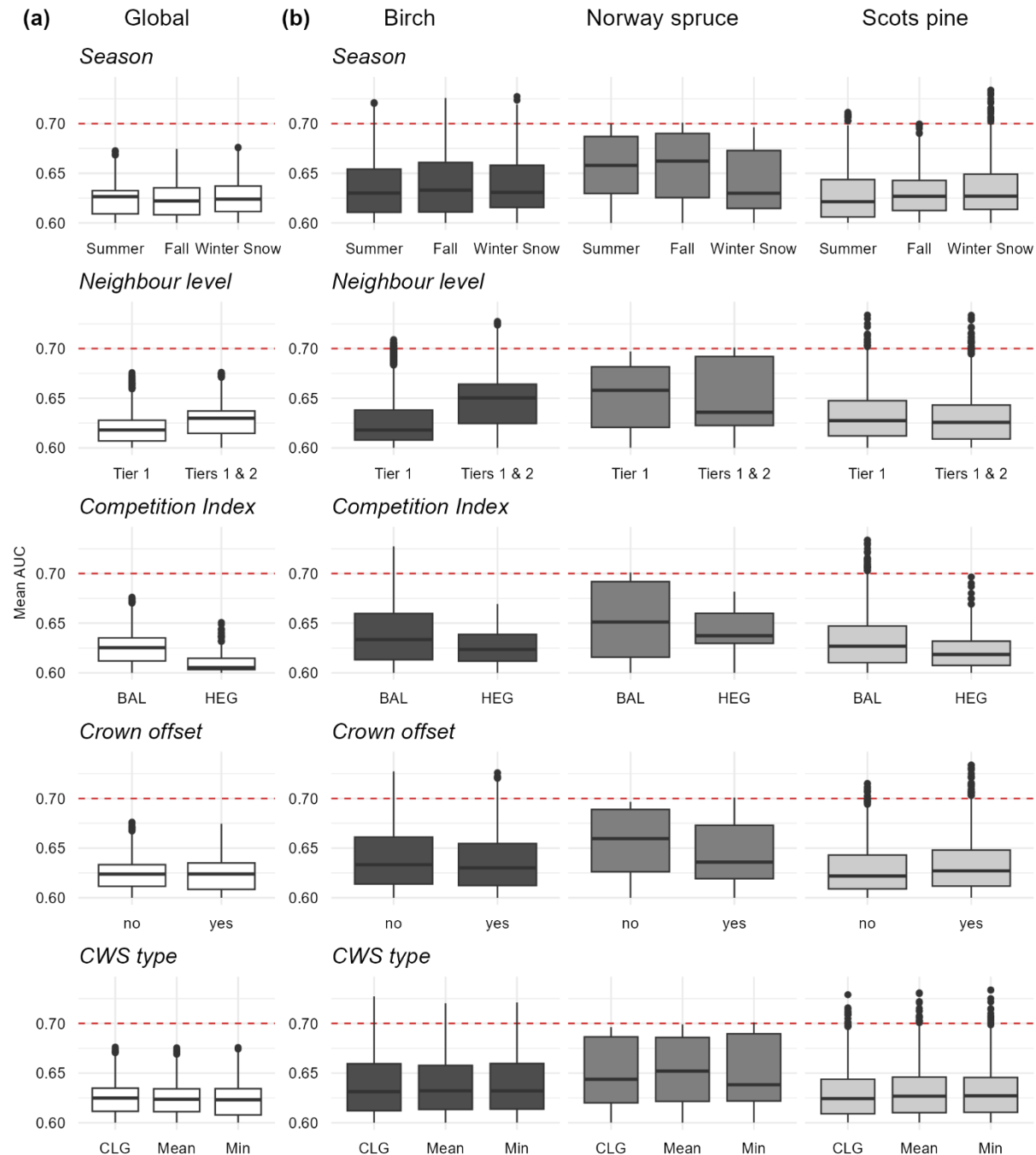
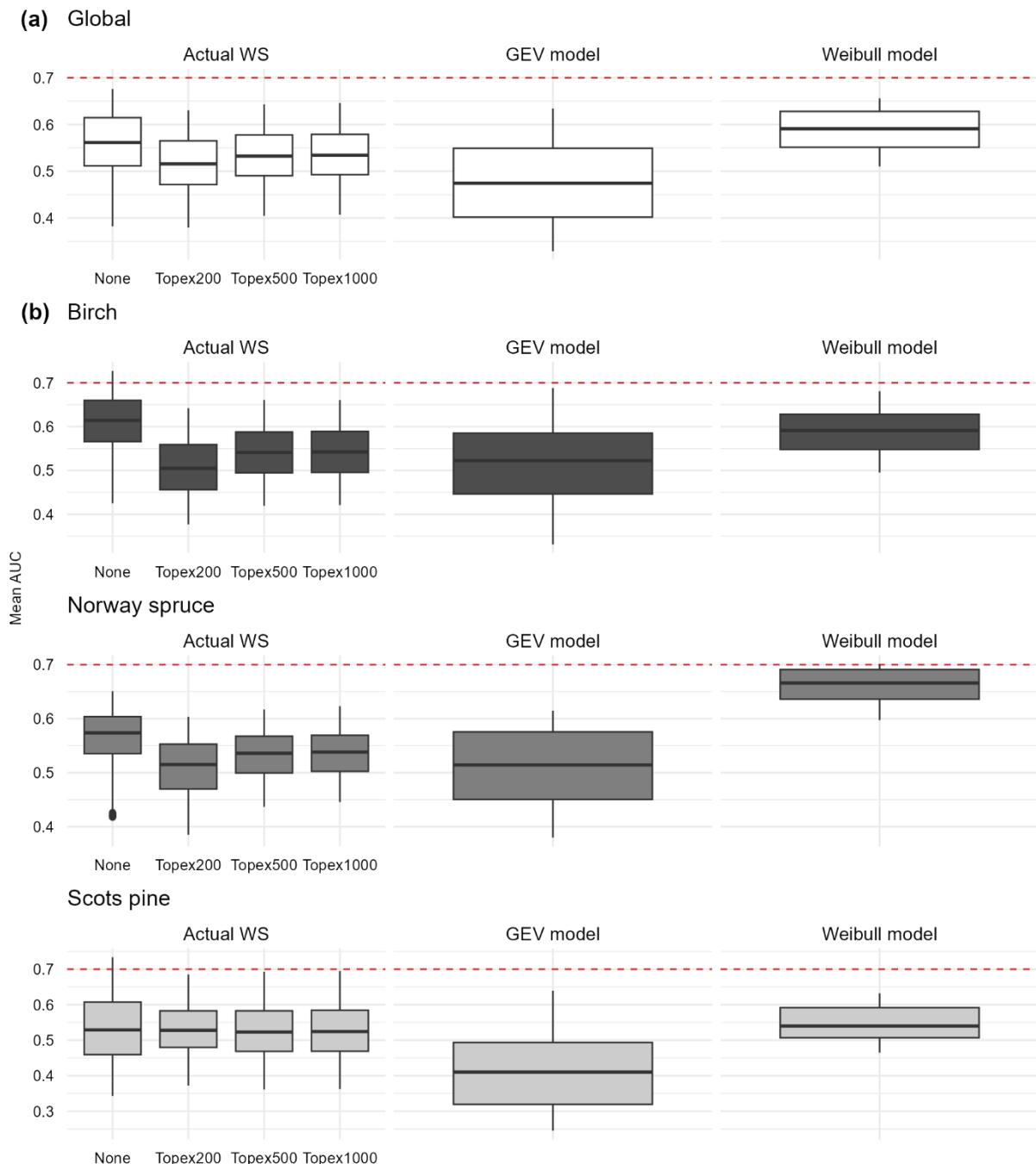


**Figure B1.** Mean AUC values of all tested global (panel a) and species-specific (panel b) models for each class of the displayed tested options. Note that the mean AUC were restricted to 0.6 and above – thus only about 20% of all tested models are included. The options are the seasonal scenario, the definition of the neighbouring trees, the type of competition index, the inclusion of a crown offset, the type of



575 Critical Wind Speed used (in relation to the choice of forest edge and gap – CLG: closest largest gap when available, Mean: mean CWS across all gap directions, Min: minimum CWS across all gap directions). The mean AUC was calculated based on 100 repeated assessments using all damaged trees with an equal number of randomly selected undamaged trees. The horizontal dotted red line shows AUC = 0.7, often taken as a threshold to represent a model with satisfactory discriminatory power. The species are further differentiated by colour: Birch in dark grey, Norway spruce in grey, and Scots pine in light grey.



580 **Figure B2.** Mean AUC values for the tested global (panel a) and species-specific (panel b) models for each class of the Wind data/model  
 581 options when calculating the probability of damage. The three main alternatives were: the use of a logistic probability function with the  
 582 actual maximum wind speed during the winter 2020-2021 (“Actual WS”) without (“None”) or with a Topex correction with different  
 583 Topex distances; the use of the Generalized Extreme Value (GEV) model fitted on the 1975-2021 time series of maximum wind speed at  
 584 each of the considered locations; or the use of the Weibull model describing the mean wind climate using the Weibull A and k parameters  
 585 extracted from the Global Wind Atlas at each of the considered locations. The mean AUC was calculated based on 100 repeated



assessments using all damaged trees with an equal number of randomly selected undamaged trees. The horizontal dotted red line shows  $AUC = 0.7$ , often taken as a threshold to represent a model with satisfactory discriminatory power. The species are further differentiated by colour: Birch in dark grey, Norway spruce in grey, and Scots pine in light grey.



590 **Table B1.** Feature importance metrics (Gain, Cover and Frequency – Freq.) of the XGBoost algorithms applied to the two alternative input datasets – ForestGALES-ML and TreeChar-ML – for each of the three wind variable alternatives. Note that the metrics presented are mean (sd) averaged across the 100 repetitions of balanced damaged/standing datasets. Abbreviations: CWS: critical wind speed; WS: wind speed; GEV: generalized extreme value. See the Materials and Methods for more information about the methods.

		<b>Gain</b>	<b>Cover</b>	<b>Freq. (%)</b>
<b>ForestGALES-ML dataset</b>	<i>Actual WS</i>			
Wind variable		0.409 (0.033)	0.393 (0.025)	38.2 (2.3)
Topex 200		0.396 (0.03)	0.453 (0.025)	45.6 (2.2)
CWS		0.195 (0.035)	0.155 (0.023)	16.1 (2.1)
	<i>1-yr return GEV</i>			
Wind variable		0.558 (0.04)	0.44 (0.03)	40.5 (2.6)
Topex 200		0.324 (0.029)	0.422 (0.028)	43.4 (2.4)
CWS		0.118 (0.036)	0.138 (0.025)	16.1 (2.4)
	<i>1-yr return Weibull</i>			
Wind variable		0.397 (0.037)	0.398 (0.03)	39.2 (2.4)
Topex 200		0.395 (0.036)	0.441 (0.029)	44.6 (2.5)
CWS		0.208 (0.033)	0.162 (0.023)	16.2 (2.2)
<b>TreeChar-ML dataset</b>	<i>Actual WS</i>			
Wind variable		0.245 (0.033)	0.207 (0.025)	18.2 (1.9)
Topex 200		0.184 (0.028)	0.203 (0.026)	17.1 (2.2)
Stand crown depth		0.126 (0.045)	0.068 (0.018)	6.3 (1.4)
Crown width		0.088 (0.028)	0.086 (0.018)	6.5 (1.4)
Stand top height		0.081 (0.041)	0.071 (0.021)	6.8 (1.5)
DBH		0.041 (0.022)	0.048 (0.02)	4.8 (1.4)
Crown depth		0.039 (0.024)	0.035 (0.014)	4.5 (1.3)
Competition index		0.038 (0.014)	0.056 (0.019)	7 (1.5)
Stand mean DBH		0.036 (0.012)	0.049 (0.013)	6.2 (1.3)
Height		0.028 (0.021)	0.038 (0.018)	3.9 (1.3)
Crown offset		0.026 (0.011)	0.042 (0.016)	5.5 (1.4)
Stand crown width		0.026 (0.012)	0.043 (0.018)	5.1 (1.4)
Spacing		0.025 (0.01)	0.036 (0.014)	5.7 (1.5)
Soil class		0.014 (0.008)	0.01 (0.005)	1.8 (0.6)
Rooting class		0.004 (0.004)	0.01 (0.008)	0.8 (0.5)
	<i>1-yr return GEV</i>			
Wind variable		0.424 (0.049)	0.269 (0.024)	21.1 (1.8)
Topex 200		0.166 (0.027)	0.189 (0.026)	16.6 (2.2)
Stand crown depth		0.08 (0.044)	0.065 (0.02)	6.2 (1.4)
Crown width		0.062 (0.024)	0.076 (0.019)	5.9 (1.4)
Stand top height		0.053 (0.031)	0.058 (0.021)	6 (1.5)
DBH		0.042 (0.023)	0.048 (0.019)	5 (1.4)
Competition index		0.031 (0.012)	0.056 (0.019)	7.3 (1.7)



Stand mean DBH	0.026 (0.011)	0.04 (0.014)	5.5 (1.4)
Crown depth	0.026 (0.02)	0.03 (0.013)	3.9 (1.2)
Stand crown width	0.022 (0.012)	0.042 (0.019)	5.1 (1.6)
Crown offset	0.02 (0.009)	0.042 (0.015)	5.5 (1.4)
Height	0.018 (0.014)	0.032 (0.014)	3.9 (1.2)
Spacing	0.018 (0.007)	0.036 (0.013)	5.6 (1.5)
Soil class	0.008 (0.005)	0.007 (0.004)	1.5 (0.7)
Rooting class	0.005 (0.004)	0.013 (0.009)	0.9 (0.6)
<i>1-yr return Weibull</i>			
Wind variable	0.193 (0.032)	0.161 (0.027)	15.7 (2.1)
Topex 200	0.177 (0.028)	0.214 (0.028)	17.6 (2.3)
Stand crown depth	0.144 (0.045)	0.085 (0.018)	7.4 (1.4)
Stand top height	0.091 (0.038)	0.077 (0.021)	7 (1.6)
Crown width	0.088 (0.029)	0.081 (0.018)	6.1 (1.4)
Stand mean DBH	0.05 (0.015)	0.068 (0.015)	7.5 (1.5)
Competition index	0.041 (0.015)	0.051 (0.017)	6.8 (1.5)
Crown depth	0.041 (0.026)	0.037 (0.015)	4.2 (1.3)
DBH	0.037 (0.02)	0.038 (0.017)	4.3 (1.3)
Height	0.033 (0.022)	0.041 (0.017)	4.2 (1.2)
Stand crown width	0.029 (0.013)	0.045 (0.018)	5.3 (1.5)
Crown offset	0.025 (0.011)	0.04 (0.015)	5.2 (1.3)
Spacing	0.023 (0.01)	0.035 (0.015)	5.1 (1.4)
Soil class	0.019 (0.01)	0.013 (0.005)	2.3 (0.7)
Rooting class	0.009 (0.007)	0.017 (0.011)	1.4 (0.7)

*Code and data availability.* The individual tree dataset is the property of eSmart Systems and thus not publicly accessible.

595 The wind and climate data are openly available at the sources indicated in the text. The code in this study is largely based on the publicly available R package fgr and can be shared upon request.

*Author contributions.* MM contributed Methodology, Formal Analysis, Software, Validation, Visualization and Writing (original draft preparation). SS contributed to Conceptualization, Funding acquisition, Methodology, Project Administration and Writing (review and editing). BG contributed to Conceptualization, Funding acquisition, Methodology, Formal analysis

600 and Writing (review and editing). TL contributed to Conceptualization, Funding acquisition, Project Administration, Resources.

*Competing interests.* The authors declare that they have no conflict of interest.



*Acknowledgements.* The authors would like to thank Magne Kaspersen (eSmart Systems, Agro Data) for leading the UAV laser scanning field campaigns in the summers 2020 and 2021 and Nhan V. Nguyen at eSmart Systems for preparing the  
605 data.

*Financial support.* The study was funded by the Norwegian Research Council for the project SkogRiskAI – “AI-based risk model for vegetation along powerlines” for the period 2020-2023 (project number 309307) and further supported by the Norwegian Research Council Contract No. 342631/L10.

## References

610 Bakkestuen, V., Erikstad, L., and Halvorsen, R.: Step-less models for regional environmental variation in Norway, *J. Biogeogr.*, 35, 1906–1922, <https://doi.org/10.1111/j.1365-2699.2008.01941.x>, 2008.

Beirlant, J., Goegebeur, Y., Teugels, J., and Segers, J.: *Statistics of Extremes: Theory and Applications*, John Wiley & Sons, Ltd, 2004.

615 Berkelaar, M.: *lpSolve: Interface to “Lp\_solve” v. 5.5 to Solve Linear/Integer Programs*, <https://doi.org/10.32614/CRAN.package.lpSolve>, 2024.

Chapman, L.: Assessing topographic exposure, *Meteorological Applications*, 7, 335–340, <https://doi.org/10.1017/S1350482700001729>, 2000.

620 Chen, T. and Guestrin, C.: XGBoost: A Scalable Tree Boosting System, in: *Proceedings of the 22nd ACM SIGKDD International Conference on Knowledge Discovery and Data Mining*, New York, NY, USA, 785–794, <https://doi.org/10.1145/2939672.2939785>, 2016.

Chen, T., He, T., Benesty, M., Khotilovich, V., Tang, Y., Cho, H., Chen, K., Mitchell, R., Cano, I., Zhou, T., Li, M., Xie, J., Lin, M., Geng, Y., Li, Y., Yuan, J., and implementation), Xgb. contributors (base Xgb.: *xgboost: Extreme Gradient Boosting*, <https://doi.org/10.32614/CRAN.package.xgboost>, 2024.

625 Chen, Y.-Y., Gardiner, B., Pasztor, F., Blennow, K., Ryder, J., Valade, A., Naudts, K., Otto, J., McGrath, M. J., Planque, C., and Luyssaert, S.: Simulating damage for wind storms in the land surface model ORCHIDEE-CAN (revision 4262), *Geoscientific Model Development*, 11, 771–791, <https://doi.org/10.5194/gmd-11-771-2018>, 2018.

Costa, M., Gardiner, B., Locatelli, T., Marchi, L., Marchi, N., and Lingua, E.: Evaluating wind damage vulnerability in the Alps: A new wind risk model parametrisation, *Agricultural and Forest Meteorology*, 341, 109660, <https://doi.org/10.1016/j.agrformet.2023.109660>, 2023.

630 Dalponte, M., Marzini, S., Solano-Correa, Y. T., Tonon, G., Vescovo, L., and Ganelle, D.: Mapping forest windthrows using high spatial resolution multispectral satellite images, *International Journal of Applied Earth Observation and Geoinformation*, 93, 102206, <https://doi.org/10.1016/j.jag.2020.102206>, 2020.

Duperat, M., Gardiner, B., and Ruel, J.-C.: Testing an individual tree wind damage risk model in a naturally regenerated balsam fir stand: potential impact of thinning on the level of risk, *Forestry: An International Journal of Forest Research*, 94, 141–150, <https://doi.org/10.1093/forestry/cpaa023>, 2021.



Dupras, J., Patry, C., Tittler, R., Gonzalez, A., Alam, M., and Messier, C.: Management of vegetation under electric distribution lines will affect the supply of multiple ecosystem services, *Land Use Policy*, 51, 66–75, <https://doi.org/10.1016/j.landusepol.2015.11.005>, 2016.

640 Eddelbuettel, D., Francois, R., Allaire, J., Ushey, K., Kou, Q., Russell, N., Ucar, I., Bates, D., and Chambers, J.: *Rcpp: Seamless R and C++ Integration.*, <https://doi.org/10.32614/CRAN.package.Rcpp>, 2023.

Gardiner, B., Byrne, K., Hale, S., Kamimura, K., Mitchell, S. J., Peltola, H., and Ruel, J.-C.: A review of mechanistic modelling of wind damage risk to forests, *Forestry: An International Journal of Forest Research*, 81, 447–463, <https://doi.org/10.1093/forestry/cpn022>, 2008.

645 Gardiner, B., Lorenz, R., Hanewinkel, M., Schmitz, B., Bott, F., Szymczak, S., Frick, A., and Ulbrich, U.: Predicting the risk of tree fall onto railway lines, *Forest Ecology and Management*, 553, 121614, <https://doi.org/10.1016/j.foreco.2023.121614>, 2024.

Garfinkel, M., Hosler, S., Roberts, M., Vogt, J., Whelan, C., and Minor, E.: Balancing the management of powerline right-of-way corridors for humans and nature, *Journal of Environmental Management*, 330, 117175, <https://doi.org/10.1016/j.jenvman.2022.117175>, 2023.

650 Gilleland, E. and Katz, R. W.: *extRemes 2.0: An Extreme Value Analysis Package in R*, *Journal of Statistical Software*, 72, <https://doi.org/10.18637/jss.v072.i08>, 2016.

Hale, S. E., Gardiner, B. A., Wellpott, A., Nicoll, B. C., and Achim, A.: Wind loading of trees: influence of tree size and competition, *Eur J Forest Res*, 131, 203–217, <https://doi.org/10.1007/s10342-010-0448-2>, 2012.

655 Hale, S. E., Gardiner, B., Peace, A., Nicoll, B., Taylor, P., and Pizzirani, S.: Comparison and validation of three versions of a forest wind risk model, *Environmental Modelling & Software*, 68, 27–41, <https://doi.org/10.1016/j.envsoft.2015.01.016>, 2015.

Hart, E., Sim, K., Kamimura, K., Meredieu, C., Guyon, D., and Gardiner, B.: Use of machine learning techniques to model wind damage to forests, *Agricultural and Forest Meteorology*, 265, 16–29, <https://doi.org/10.1016/j.agrformet.2018.10.022>, 2019.

660 Hegyi, F.: A simulation model for managing jack pine stands, in: *Growth Models for Tree and Stand Simulation*, Royal Coll. For., Stockholm, 74–90, 1974.

Hernangómez, D.: Using the tidyverse with terra objects: the tidyterra package, *Journal of Open Source Software*, 8, 5751, <https://doi.org/10.21105/joss.05751>, 2023.

Hijmans, R. J.: *terra: Spatial Data Analysis*, <https://doi.org/10.32614/CRAN.package.terra>, 2024.

665 Hosmer, D. W., Lemeshow, S., and Sturdivant, R. X.: *Applied Logistic Regression*, in: *Applied Logistic Regression*, John Wiley & Sons, Ltd, 510, <https://doi.org/10.1002/9781118548387.fmatter>, 2013.

IEA: Electricity security in tomorrow's power systems, IEA, 2020.

670 Jahani, A. and Saffariha, M.: Tree failure prediction model (TFPM): machine learning techniques comparison in failure hazard assessment of *Platanus orientalis* in urban forestry, *Nat Hazards*, 110, 881–898, <https://doi.org/10.1007/s11069-021-04972-7>, 2022.



Jain, A., Shah, T., Yousefhussien, M., and Pandey, A.: Combining Remotely Sensed Imagery with Survival Models for Outage Risk Estimation of the Power Grid, in: 2021 IEEE/CVF Conference on Computer Vision and Pattern Recognition Workshops (CVPRW), 2021 IEEE/CVF Conference on Computer Vision and Pattern Recognition Workshops (CVPRW), 1202–1211, <https://doi.org/10.1109/CVPRW53098.2021.00131>, 2021.

675 Jenkinson, A. F.: The frequency distribution of the annual maximum (or minimum) values of meteorological elements, Quarterly Journal of the Royal Meteorological Society, 81, 158–171, <https://doi.org/10.1002/qj.49708134804>, 1955.

Kamimura, K., Gardiner, B., Dupont, S., Guyon, D., and Meredieu, C.: Mechanistic and statistical approaches to predicting wind damage to individual maritime pine (*Pinus pinaster*) trees in forests, Can. J. For. Res., 46, 88–100, <https://doi.org/10.1139/cjfr-2015-0237>, 2016.

680 Kassambara, A.: ggpubr: “ggplot2” Based Publication Ready Plots, , <https://doi.org/10.32614/CRAN.package.ggpubr>, 2023.

Kennedy, F.: The identification of soils for forest management, Edinburgh: Forestry Commission Publications, 2002.

Krisans, O., Matisons, R., Rust, S., Burnevica, N., Bruna, L., Elferts, D., Kalvane, L., and Jansons, A.: Presence of Root Rot Reduces Stability of Norway Spruce (*Picea abies*): Results of Static Pulling Tests in Latvia, Forests, 11, 416, <https://doi.org/10.3390/f11040416>, 2020.

685 Lehtonen, I., Hoppula, P., Pirinen, P., and Gregow, H.: Modelling crown snow loads in Finland: a comparison of two methods, Silva Fenn., 48, <https://doi.org/10.14214/sf.1120>, 2014.

Li, J., Liu, L., Liang, Y., He, C., and Jin, J.: An Integrated Estimating Approach for Design Wind Speed under Extreme Wind Climate in the Yangtze River Inland Waterway, Atmosphere, 13, 1849, <https://doi.org/10.3390/atmos13111849>, 2022.

690 Liu, Z., Peng, C., Work, T., Candau, J.-N., DesRochers, A., and Kneeshaw, D.: Application of machine-learning methods in forest ecology: recent progress and future challenges, Environ. Rev., 26, 339–350, <https://doi.org/10.1139/er-2018-0034>, 2018.

Locatelli, T., Gardiner, B., Tarantola, S., Nicoll, B., Bonnefond, J.-M., Garrigou, D., Kamimura, K., and Patenaude, G.: Modelling wind risk to *Eucalyptus globulus* (Labill.) stands, Forest Ecology and Management, 365, 159–173, <https://doi.org/10.1016/j.foreco.2015.12.035>, 2016.

695 Locatelli, T., Tarantola, S., Gardiner, B., and Patenaude, G.: Variance-based sensitivity analysis of a wind risk model - Model behaviour and lessons for forest modelling, Environmental Modelling & Software, 87, 84–109, <https://doi.org/10.1016/j.envsoft.2016.10.010>, 2017.

Locatelli, T., Gardiner, B., Hale, S., and Nicoll, B.: fgr: r Version of the ForestGALES wind risk model. R package version 1.0, 2022.

700 Lorenz, R., Becker, N., Gardiner, B., Ulbrich, U., Hanewinkel, M., and Benjamin, S.: Storm damage beyond wind speed – Impacts of wind characteristics and other meteorological factors on tree fall along railway lines, EGUsphere, 1–34, <https://doi.org/10.5194/egusphere-2024-120>, 2024.

705 Merlin, M., Locatelli, T., Gardiner, B., and Astrup, R.: Large-scale modelling wind damage vulnerability through combination of high-resolution forest resources maps and ForestGALES, Forest Ecosystems, 14, 100361, <https://doi.org/10.1016/j.fecs.2025.100361>, 2025.



Morimoto, J., Aiba, M., Furukawa, F., Mishima, Y., Yoshimura, N., Nayak, S., Takemi, T., Chihiro, H., Matsui, T., and Nakamura, F.: Risk assessment of forest disturbance by typhoons with heavy precipitation in northern Japan, *Forest Ecology and Management*, 479, 118521, <https://doi.org/10.1016/j.foreco.2020.118521>, 2021.

710 Nicoll, B. C., Gardiner, B. A., Rayner, B., and Peace, A. J.: Anchorage of coniferous trees in relation to species, soil type, and rooting depth, *Can. J. For. Res.*, 36, 1871–1883, <https://doi.org/10.1139/x06-072>, 2006.

NVE: Trær til besvær. Lærdommer om skogrydding i etterkant av ekstremværet Dagmar, Norges vassdrags- og energidirektorat NVE, 2012.

715 Öhman, K., Llorente, I. P., Fustel, T., Bohlin, I., Lämås, T., and Eggers, J.: Integrating wind damage vulnerability into long-term forest planning: An optimisation-based model for spatial decision support, *Trees, Forests and People*, 20, 100870, <https://doi.org/10.1016/j.tfp.2025.100870>, 2025.

Palutikof, J. P., Brabson, B. B., Lister, D. H., and Adcock, S. T.: A review of methods to calculate extreme wind speeds, *Meteorological Applications*, 6, 119–132, <https://doi.org/10.1017/S1350482799001103>, 1999.

720 Patacca, M., Lindner, M., Lucas-Borja, M. E., Cordonnier, T., Fidej, G., Gardiner, B., Hauf, Y., Jasinevičius, G., Labonne, S., Linkevičius, E., Mahnken, M., Milanovic, S., Nabuurs, G.-J., Nagel, T. A., Nikinmaa, L., Panyatov, M., Bercak, R., Seidl, R., Ostrogović Sever, M. Z., Socha, J., Thom, D., Vuletic, D., Zudin, S., and Schelhaas, M.-J.: Significant increase in natural disturbance impacts on European forests since 1950, *Glob. Chang. Biol.*, 29, <https://doi.org/10.1111/gcb.16531>, 2022.

Pawlik, Ł. and Harrison, S. P.: Modelling and prediction of wind damage in forest ecosystems of the Sudety Mountains, SW Poland, *Science of The Total Environment*, 815, 151972, <https://doi.org/10.1016/j.scitotenv.2021.151972>, 2022.

725 Poulos, H. M. and Camp, A. E.: Decision support for mitigating the risk of tree induced transmission line failure in utility rights-of-way, *Environmental Management*, 45, 217–226, <https://doi.org/10.1007/s00267-009-9422-5>, 2010.

Quine, C. P.: Estimation of mean wind climate and probability of strong winds for wind risk assessment, *Forestry: An International Journal of Forest Research*, 73, 247–258, <https://doi.org/10.1093/forestry/73.3.247>, 2000.

R Core Team: R: A Language and Environment for Statistical Computing, 2024.

730 Reder, S., Kruse, M., Miranda, L., Voss, N., and Mund, J.-P.: Unveiling wind-thrown trees: Detection and quantification of wind-thrown tree stems on UAV-orthomosaics based on UNet and a heuristic stem reconstruction, *Forest Ecology and Management*, 578, 122411, <https://doi.org/10.1016/j.foreco.2024.122411>, 2025.

Avbrotsstatistikk fra Reguleringsmyndigheita for energi - NVE: <https://www.nve.no/reguleringsmyndigheten/publikasjoner-og-data/statistikk/avbrotsstatistikk/>, last access: 19 May 2025.

735 Rouault, E., Warmerdam, F., Schwehr, K., Kiselev, A., Butler, H., Łoskot, M., Szekeres, T., Tourigny, E., Landa, M., Miara, I., Elliston, B., Kumar, C., Plesca, L., Morissette, D., Jolma, A., and Dawson, N.: GDAL, <https://doi.org/10.5281/zenodo.6517191>, 2022.

740 Sey, N. E. N., Amo-Boateng, M., Domfeh, M. K., Kabo-Bah, A. T., and Antwi-Agyei, P.: Deep learning-based framework for vegetation hazard monitoring near powerlines, *Spat. Inf. Res.*, 31, 501–513, <https://doi.org/10.1007/s41324-023-00518-0>, 2023.



Soukissian, T. H. and Tsalis, C.: The effect of the generalized extreme value distribution parameter estimation methods in extreme wind speed prediction, *Nat Hazards*, 78, 1777–1809, <https://doi.org/10.1007/s11069-015-1800-0>, 2015.

745 Stadelmann, C., Grottian, L., Natkhan, M., and Sanders, T. G.: Improving the predictive capacity of the windthrow risk model ForestGALES with long-term monitoring data – A statistical calibration approach, *Forest Ecology and Management*, 576, 122389, <https://doi.org/10.1016/j.foreco.2024.122389>, 2025.

Stage, A. R.: Prognosis model for stand development, *Intermountain Forest & Range Experiment Station, Forest Service, U.S. Dept. of Agriculture*, Ogden, Utah, <https://doi.org/10.5962/bhl.title.69018>, 1973.

750 Straker, A., Puliti, S., Breidenbach, J., Kleinn, C., Pearse, G., Astrup, R., and Magdon, P.: Instance segmentation of individual tree crowns with YOLOv5: A comparison of approaches using the ForInstance benchmark LiDAR dataset, *ISPRS Open Journal of Photogrammetry and Remote Sensing*, 9, 100045, <https://doi.org/10.1016/j.ophoto.2023.100045>, 2023.

Szymczak, S., Bott, F., Babeck, P., Frick, A., Stöckigt, B., and Wagner, K.: Estimating the hazard of tree fall along railway lines: a new GIS tool, *Nat Hazards*, 112, 2237–2258, <https://doi.org/10.1007/s11069-022-05263-5>, 2022.

755 Walker, M. and Dahle, G. A.: Literature Review of Unmanned Aerial Systems and LIDAR with Application to Distribution Utility Vegetation Management, Arboriculture & Urban Forestry (AUF), 49, 144–156, <https://doi.org/10.48044/jauf.2023.011>, 2023.

Wickham, H.: *ggplot2*, Springer International Publishing, Cham, <https://doi.org/10.1007/978-3-319-24277-4>, 2016.

Žemaitis, P., Armoška, E., Stakėnas, V., and Kulbokas, G.: Wood decay and Norway spruce vulnerability to wind-inflicted mortality in monospecific and mixed stands in hemiboreal forests, *Forest Ecology and Management*, 569, 122163, <https://doi.org/10.1016/j.foreco.2024.122163>, 2024.

760 Zubkov, P., Gardiner, B., Nygaard, B. E., Guttu, S., Solberg, S., and Eid, T.: Predicting snow damage in conifer forests using a mechanistic snow damage model and high-resolution snow accumulation data, *Scandinavian Journal of Forest Research*, 39, 59–75, <https://doi.org/10.1080/02827581.2023.2289660>, 2024.